Fiber-Optic Temperature Sensor Design Adapted for Libyan Environment

Mohammed Bin Saeed[1*], Mohamed Otman Twati[2]

bin703m@gmail.com[1], M.twati@uot.edu.ly[2]

[1, 2] Department of Electrical and Electronic Engineering, University of Tripoli, Libya

*Corresponding author email: bin703m@gmail.com

ABSTRACT

In this work, the design of the Fiber optic Temperature Sensor has been performed using two different techniques aimed at determining the optimum design parameters of the fiber optic sensor that should work properly in the Libyan environment (temperature: -13 to 57.8 degrees Celsius). The first technique is based on Fabry-Perot Interferometer that tracks the phase change of the received light by the interferometer due to the sensitivity of the Fabry-Perot's cavity to the surrounding temperature changes. Three different substances (GaAs, Ge and Si) were used in determining the optimum design parameters of the fiber optic sensor. The optical wavelength used is 1550nm with line width of 40nm. The material selected is Si where the optimum Fabry-Perot length was found to be 20.7μm. The second technique studied is based on Fiber Coupling Actuated by a Bimetal Strip to read the change in temperature with respect to coupling power loss. Three different standard Bimetal types were used for the design of the strip, (KANTAL 200 TB20110 Ni/MnNiCu), (KANTAL 135 Ni/NiMn-steel) and (KANTAL100 TB0965 Ni/NiMn-steel). The (KANTAL 200 TB20110 Ni/MnNiCu) Bimetal material was selected for the optimal sensor design. The optimum design length, delta deflection and thickness for the strip were found to be 5.6μm, 35μm and 1.3μm respectively.

1   Introduction

Over the last few decades, optical fibers have been widely deployed in telecommunication industries owing to their special performance as the best light guidance. Optical fibers have been intensively investigated at various sensor fields, owing to their unique characteristics such as multiplexing, remote sensing, high flexibility, low propagating loss, high sensitivity and low fabrication cost. Temperature is one of the most widely measured parameters within safety industry and science. In many applications, sensors are required, because of their immunity to electromagnetic interference, small in size, suitability for remoting and having lightweight. In addition, they allow operation in harsh environments to replace conventional electronic

sensors due to their possibility of performing measurements in environments suffering from electromagnetic disturbance, or in environments where electronics cannot survive. Fiber optic sensors can survive offer an excellent solution to many of these challenges. Different fiber optic sensor techniques have been designed and many researches are focused on developing reliable and cost-effective fiber temperature sensors. In this work, we first describes Fabry-Perot interferometer temperature sensor that uses a reflective etalon. The etalon's optical path difference (OPD) is a temperature dependent. This is due, primarily, to the dependence of its refractive index to the temperature variations. The sensed temperature can then be determined from the positions of the minima in the sensor's output spectrum by several simple types of spectrum analyzers, other type of sensing devices that use power coupling loss between two fibers to determine the temperature, will be described next. The designed fiber-optic temperature sensors would be used highly in high power generation rooms.

2   Materials and Methods

Fabry-Perot Interferometer

Basically, the Fabry-Perot temperature sensor (FPI) is a thin platelet of a material that has a temperature-dependent refractive index [1]. It is composed of two parallel reflecting surfaces separated by a certain distance called etalon and are classified into two categories: one is extrinsic and the other is intrinsic [2], [3]. The extrinsic FPI sensor uses the reflections from an external cavity formed out of the interesting fiber [4]. Figure 1 (a) shows an extrinsic FPI sensor, in which the air cavity is formed by a supporting structure. Since it can utilize high reflecting mirrors, the temperature-sensitive interferometer is constructed from thin films that are deposited directly onto the end of an optical fiber [5]. In other sense, when the cavity material is not the fiber itself, it is called extrinsic and it is shown in Figure 1 (b). Figure 2 shows a more detailed Fiber-optic temperature sensor using a thin-film Fabry-Perot interferometer.
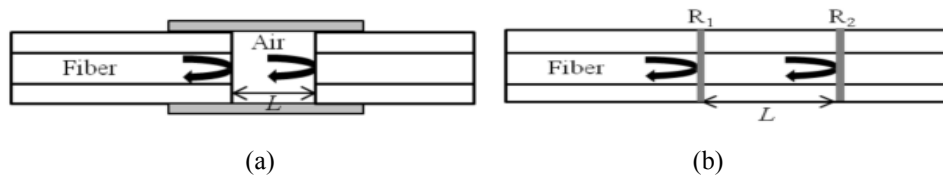

| (a) | (b) |

Figure 1: (a) Extrinsic FPI sensor made by forming an external air cavity, and (b) intrinsic FPI sensor formed by two reflecting components, R1 and R2, along a fiber.
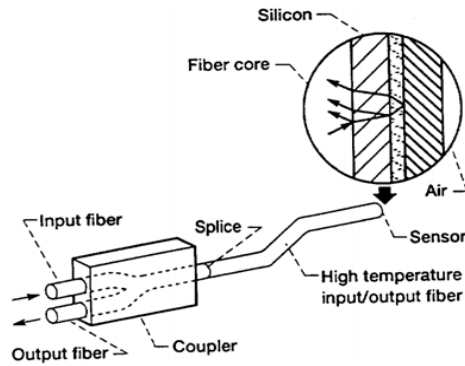
Figure 2: Fiber-optic temperature sensor using a thin-film Fabry-Perot interferometer.

2.2 Fiber Coupling Actuated by a Bimetal Strip

Coupling based intensity modulated fiber-optic sensors can be configured in basically two ways: either in a reflective arrangement as shown in Figure 3 (a), or in a transmissive arrangement, using straightforward transmission from one fiber to the other, as in Figure 3 (b).
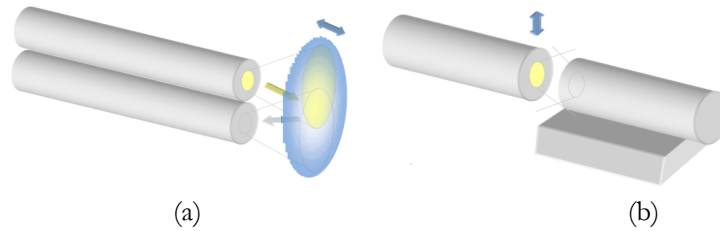

(a)   (b)

Figure 3: (a) Schematic view of a coupling based intensity modulated fiber-optic sensor using a reflective configuration (b) using a transmissive configuration.

The bimetal strip Consists of different metals expand at different rates as they warm up, behave in different manner when exposed to temperature variation owing to their different thermal different thermal expansion rates. One end of straight bimetallic strip is fixed in place as the strip is heated the other end tends to curve away from, the side that has the greater coefficient of linear expansion as shown in Figure 4.
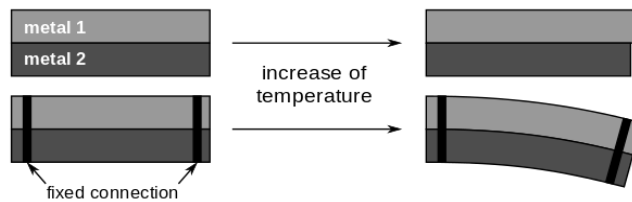

Figure 4: Shows the bimetal strip.

This part should contain sufficient detail to reproduce reported data. It can be divided into subsections if several methods are described. Methods already published should be indicated by a reference [4], only relevant modifications should be described.

3   Theory and Calculation

Fabry-Perot Interferometer

Here, the interferometer's optical path difference (OPD) is given by:

$$\Lambda_{OPD} = 2n_1 L \cos\theta_1 \tag{1}$$

And:

$$\Phi = \frac{2\pi}{\lambda}\Lambda_{OPD} \tag{2}$$

As shown if the length, L, of the cavity increases the phase shift, Φ, between two reflected light increases as well as refractive index of the material n_1. the reflectivity can be rewritten as:

$$R_F = \frac{F\sin\Phi^2}{1 + F\sin\Phi^2} \tag{3}$$

Where:

$$F = \frac{4R}{(1-R)^2} \tag{4}$$

With:

$$R = \frac{(n_1 - n_2)^2}{(n_1 + n_2)^2} \tag{5}$$

The transmissivity of the ideal Fabry-Perot interferometer is given by:

$$T_F = \frac{1}{1 + F\sin\Phi^2} \tag{6}$$

As expected, for zero loss, $T_F + R_F = 1$, Figure 5 shows that for (GaAs) for designed length as function (Φ)[7].
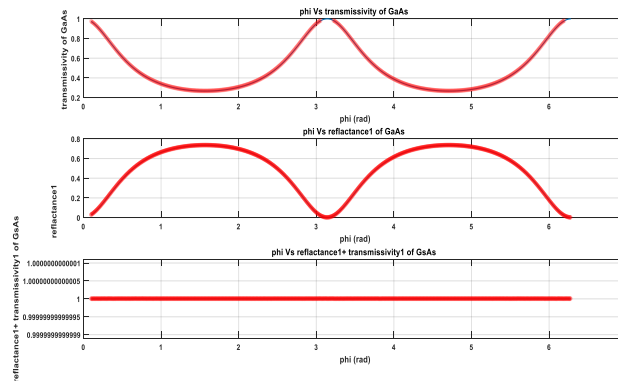

Figure 5: (Reflectance + Transmissivity) GaAs for designed length as function of (Φ).

Fiber Coupling Actuated by a Bimetal Strip

The temperature dependent deflection δ of a bimetal strip clamped at one end is given by:

$$\delta = \alpha_d \cdot (T - T_0) \frac{{L_0}^2}{t} \qquad (7)$$

Where α_d is the specific deflection, T represents the variable the temperature, L_0 is the free strip length at room temperature T_0 and t represents the strip thickness. For a fiber sensor configuration according to Figure 6
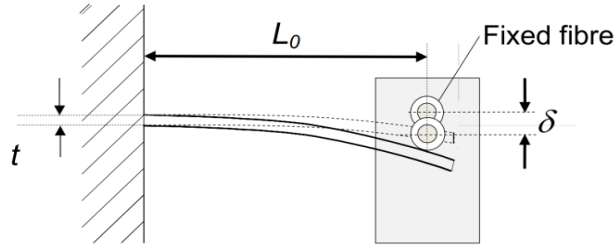

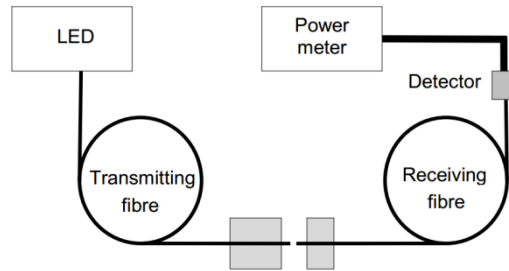**Figure 6:** Temperature sensor operation principle.

Figure 7: Temperature sensor operation principle.

In the linear temperature region of the bimetal strip, the deflection can be counted from any reference temperature T_0, which means that the reference temperature could be chosen when the moveable fiber has a zero offset to the fixed fiber. The coupled power P between two fibers as a function of temperature T [8], can thus be written as:

$$P(T) = P_0 \cdot e^{-k(T-T_0)^2} \qquad (8)$$

A Theory section should extend, not repeat, the background to the article already dealt with in the Introduction and lay the foundation for further work. In contrast, a Calculation section represents a practical development from a theoretical basis.

4 Results and Discussion

4.1 Fabry-Perot Interferometer

The design consists of the selection of a material (GaAs, Ge, Si) and the determination of the optimum thickness at for the Libyan environment range, the interferometer's reflectance is minimized at resonance, or $\Phi = \pi m$, where m is an integer. For the ideal Fabry-

Perot interferometer, the minimum reflectance $[R_F]_{min} = 0$. In terms of wavelength, the resonance condition is at $\lambda = \lambda_m$ where:

$$m\lambda_m = \Lambda_{OPD} \tag{9}$$

The maximum reflectance, which occurs at $\Phi = \pi(m+1/2)$ and is given by:

$$[R_F]_{max} = \frac{F}{1 + F} \tag{10}$$

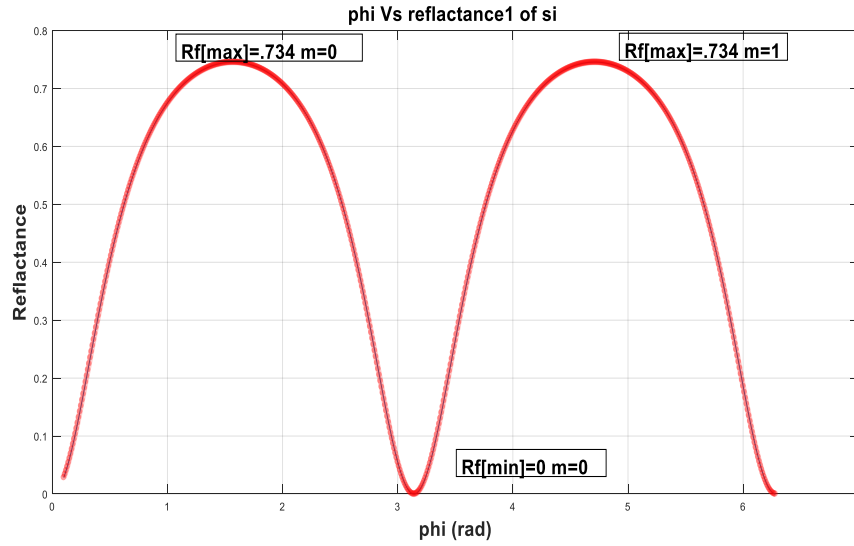**Figure 8:** Shows the reflectance of (GaAs) for designed length (20.7 µm).

The maximum reflectance obtained for the designed length, L=20.7 µm, is equal 0.734, for the integers m=0, 1, 2 as shown in Figure 8. The phase sensitivity is obtained by differentiating equation (3), which gives:

$$\frac{dR_F}{d\Phi} = \frac{F \sin 2\Phi}{(1 + F \sin \Phi^2)^2} \tag{11}$$
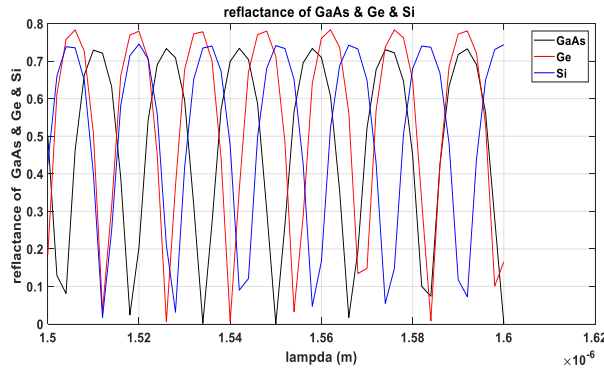

Figure 9: Comparison of phase sensitivity of (GaAs) & (Ge) & (Si) as function of (λ).
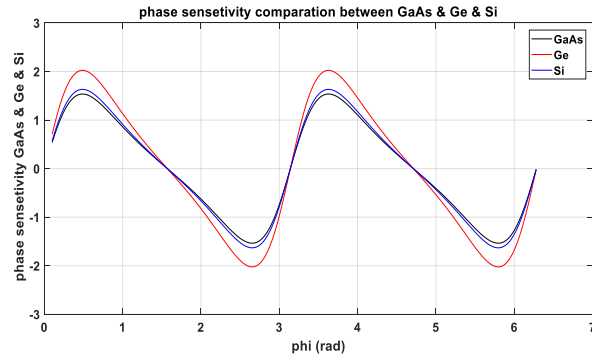
Figure 10: Comparison of phase sensitivity of (GaAs) & (Ge) & (Si) as function of Φ.

The temperature sensitivity of the Fabry-Perot's phase shift is given by:

$$\frac{d\Phi}{dT} = \pi \frac{\Lambda_{OPD}}{\lambda} \kappa_\Phi \tag{12}$$
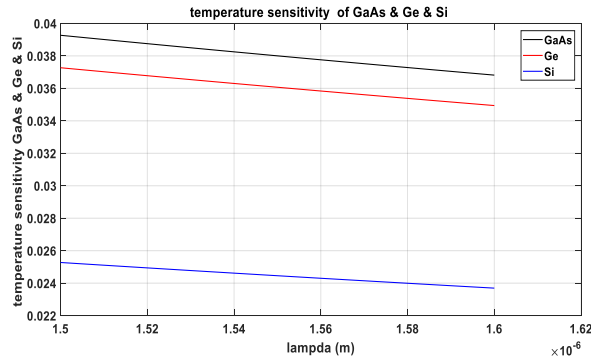
Figure 11: Comparison of temperature sensitivity of the Fabry-Perot's phase shift of (GaAs) & (Ge) & (Si) as function of λ and L=20.7μm.

By integrating both sides $\int d\Phi = \int \pi \frac{\Lambda_{OPD}}{\lambda} \kappa_\Phi . dT, \Phi = \pi \frac{\Lambda_{OPD}}{\lambda} \kappa_\Phi . T$

Figure 12: Phase vs. Temperature.

Where:

$$\kappa_\Phi = \kappa_n + \kappa_L \tag{13}$$

Here, κ_n is the thermo-optic coefficient

$$\kappa_n = \frac{1}{n_1}\frac{dn_1}{dT} \tag{14}$$

And κ_L is the thermal expansion coefficient,

$$\kappa_L = \frac{1}{L}\frac{dL}{dT} \tag{15}$$

The temperature sensitivity of the Fabry-Perot's reflectance can be determined by substituting from equations (11) and (12) into:

$$\frac{dR_F}{dT} = \left(\frac{dR_F}{d\Phi}\right)\left(\frac{d\Phi}{dT}\right) \tag{16}$$

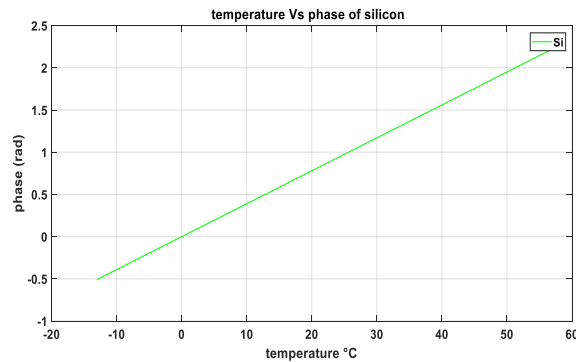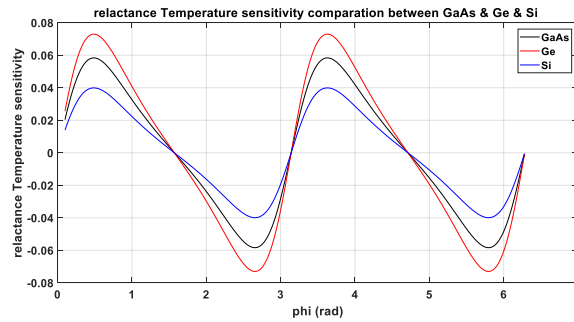**Figure 13:** Comparison of temperature sensitivity of the Fabry-Perot's reflectance of (GaAs) & (Ge) & (Si) as function of(Φ).

(Ge) gave us best results for temperature sensitivity of the Fabry-Perot's reflectance because it has the largest refractive index [7].

Selection of Temperature Sensitive Material

G. Beheim has previously summarized a comparison of candidate materials for a thin-film temperature sensor. The temperature sensitivity of various candidate materials requires that sensitivity figure-of-merit be independent of the film thickness, Table1 tabulates the candidate materials in descending order of κ_Φ. This table provides n, κ_n, and κ_L, together with the wavelengths at which the optical properties were measured, all data.

Table 1: Properties of candidate Fabry-Perot materials. Units of κ_n, κ_L, and κ_Φ are $10^{-6}/0C$.

Material	λ (μm)	n	κ_n	κ_L	κ_Φ
GaAs	0.9	3.6[7]	120[7]	5.7[5]	126
Ge	2.55	4.06[7]	100[7]	5.7[7]	106
Si	2.5	3.44	46[7]	2.6[7]	
	1.5	3.5	53[7]		
	1.26	3.51[7]	59[7]		
	0.78	3.695[7]	76[7]		79

So the temperature induced phase change is almost entirely caused by the change in refractive index. Of the three materials with the largest values of κ_Φ, silicon is best suited for this range

application and available almost everywhere, however, it is highly absorbing at the emission wavelengths of AlGaAs LEDs. At 830nm, the absorption coefficient of germanium is 4.5×104 cm^{-1}, so that transmission through 1 μm produces a 20-dB loss. At 1.3μm, is much lower, 0.68×104 cm^{-1}, but this wavelength is outside the range of inexpensive silicon photodiodes, Silicon is preferred to germanium for this application, because its absorption coefficient is much lower at the AlGaAs emission wavelengths. At 830nm, α=0.19×104 cm^{-1}, which causes a 17% absorption in 1.0μm [6].

Determination of Fabry-Perot Sensor's Thickness

For a typical AlGaAs's LED we can choose any LED, $\frac{\Delta\lambda_{LED}}{\lambda_m} \geq \frac{\lambda_m}{2\Lambda_{OPD}}$, $\Lambda_{OPD} = m \times \lambda_m$, λ=1550nm and $\Delta\lambda_{LED}$= 40nm, which gives m≥19.3. For silicon, this corresponds to L1≥4 μm.

$$m \leq \frac{1}{\kappa_\Phi (T_{max} - T_{min})} \tag{17}$$

For a silicon sensor with a -13 to 57.80 °C.

$$\Lambda_{OPD}/\lambda_m \leq \frac{1}{79 \times 10^{-6}(57.8-(-13))} = \frac{2 \times 3.695 \times L \times \cos(3.1)}{1550 \times 10^{-9}} \leq \frac{1}{79 \times 10^{-6}(57.8-(-13))}$$

$$L \leq \frac{1550 \times 10^{-9}}{2 \times 3.695 \times \cos(3.1) \times 79 \times 10^{-6}(57.8-(-13))} = 37.55\mu m, \text{ must be less than } 178.7\mu m, \text{ which gives}$$

L<.37.55μm. In this case we chose L1= 20.7μm, so that L1 is within the above limiting cases so the optimization length is 20.7μm.

4.2 Fiber Coupling Actuated by a Bimetal Strip

First we should measure P_0, the coupled power, at temperature T_0, i.e., at zero offset (deflection), the moveable fiber at zero position, the design factor k is given by :

$$k = (\frac{\alpha_d}{w} \cdot \frac{L_0^2}{t})^2 \tag{18}$$

where *w* is the characteristic radius of the modulation function of the sensor and typically 25μm, the temperature dependent loss **A** of the sensor, quoted in decibels (dB), can be derived as

$$A(T) = 10 . \log \frac{p(T_0)}{p(T)} = K . (T - T_0)^2 \tag{19}$$

Using equations (18) and (19) the design constant **K** can be written as:

$$K = (\frac{\alpha_d}{w} \cdot \frac{L_0^2}{t})^2 . 10 \log e \tag{20}$$

Using formulas (7), (19) and (20) a temperature sensor for any temperature range in the linear region of the bimetal can be designed, The sensitivity of such a sensor can be adjusted by choosing a suitable bimetal (parameters α_d and t) and by adjusting the free strip length L_0, T_0 should therefore be chosen to be a bit lower than the minimum temperature T_{min} to be

measured, or a bit larger than the maximum temperature T_{max} also to be measured. The deflection range Δ is given by:

$$\Delta = \delta_{\mathbf{m}} - \delta_{\mathbf{min}} = \frac{\alpha_d L_0{}^2}{t} \cdot (T_{max} - T_{min}) \qquad (21)$$

Where δ_m is the desired maximum deflection and T_{max} and T_{min} are the maximum and minimum temperatures of the measurement range, corresponding to the desired deflection range. From equation (21) the fiber position L_0 can be calculated, and using this value together with $\delta = \delta_{min}$ and $T=T_{min}$, equation (7) gives the zero deflection temperature T_0 for the right slope of the modulation curve. First we take three material with linear range that can measure our Libyan environment with specific deflection (20.8x10⁻⁶, 13.9x10⁻⁶, 10x10⁻⁶), as shown in Table 2. In designing and calculating sensor's parameters we take the larger deflection range to increase the sensitivity, this is because our temperature range is large.

Table 2: Some details of standard bimetal types

Thermostatic Bimetal type DIN designation	added	Specific deflection [10⁻⁶ K⁻¹]	Specific curvature [10⁻⁶ K⁻¹]	Linearity range [°C]	Max operating temperature [°C]	Resistivity [Ω mm² m⁻¹] at temperature °C						Thermal conductivity [Wm⁻¹ °C⁻¹]	Modulus of elasticity [103 N mm⁻²]	Standard hardness [HV] low exp. side	high exp. side	Density [g cm⁻³]
						0	20	100	200	300	400					
230		22.7	43.0	-20−+230	330	1.04	1.05	1.15	1.22	1.28		6	135	210	200	7.8
200	TB20110	20.8	39.0	-20−+175	330	1.09	1.10	1.20	1.27	1.33		6	135	210	250	7.8
155	TB1577A	15.6	28.5	-20−+250	450	0.77	0.78	0.86	0.94	1.00	1.07	13	170	210	260	8.1
145		14.8	27.7	-20−+250	450	0.78	0.79	0.85	0.93	0.99	1.06	12	170	210	240	8.1
135		13.9	25.9	-20−+200	450	0.78	0.79	0.85	0.93	0.99	1.06	12	170	210	240	8.1
130		13.2	24.8	-20−+325	450	0.72	0.74	0.82	0.89	0.95	1.02	12	170	210	240	8.1
115	TB1170	11.7	22.0	-20−+380	450	0.68	0.70	0.78	0.86	0.93	0.99	13	170	210	240	8.1
100	TB0965	10.0	18.6	-20−+425	450	0.62	0.65	0.75	0.86	0.94	1.00	15	175	210	240	8.2
94S		9.5	17.8	-0−+200	450	0.84	0.85	0.90	0.95			12	190	210	250	8.1
60		6.0	11.3	-20−+450	450	0.19	0.21	0.28	0.37	0.47	0.59	44	190	230	240	8.0
50HT		5.0	9.4	-20−+500	550	0.635	0.66	0.72	0.78	0.83		20	200	240	340	7.8

Table 3: Bimetal data and calculated sensor design parameters for minimum deflection = 5 μm, T_{min}=-13 °C and T_{max}= 57.8 °C using a fiber coupling with a typical characteristic radius of w= 25μm.

Type	α_d (10⁻⁴ K⁻¹)	t (mm)	Δ (μm)	L_0 (mm)	T_0 (°C)	K (10⁻ ³dB K⁻²)	$A(T_{min})$ (10⁻³dB)	$A(T_{max})$ (dB)
200	20.8	1.3	20	4.2	-15	0.55	2.2	2.938
			25	4.7	-18	0.86	21.7	4.978
			35	5.6	-20	1.7	83.2	10.278
			40	5.9	60	2.2	11819.6	.0107
135	13.9	0.8	20	4	-15	0.55	2.2	2.938
			25	4.5	-18	0.86	21.7	4.978
			35	5.3	-20	1.7	83.2	10.278
100	10	1.0	10	5.3	-15	0.55	2.2	2.938
			16	5.9	-18	.86	21.7	4.978
			25	7	-20	1.7	83.2	10.278

The sensitivity of the sensor in terms of the loss change in dB per temperature degree is given by the derivative of:

$$s(T) = \frac{d(A)}{d(T)} = 2.K.(T - T_0) \tag{22}$$

By integrate both sides $\int d(A) = \int 2KTd(T) - \int 2KT_0d(T)$

$A = KT^2 - 2KT_0T$.   Fig.14 shows the sensitivity versus the temperature at different deltas, whereas the comparison between the two devices is shown in Fig. 15.
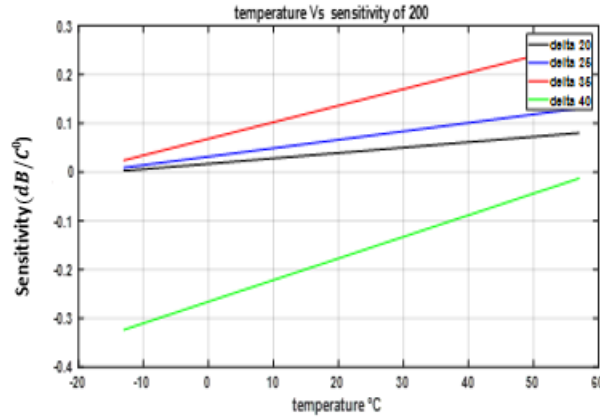

Figure 14: Sensitivity as a function of temperature for the sensor designs based on type200 bimetal listed in Table 3.

Table 3 shows the different material and the different design parameters, where the best design parameters obtained are at length of 5.6 mm and at Δ=35μm.

Clearly, Fabry-Perot technique sensor is more accurate than Intensity-type Fiber Optic Sensor, because the Fabry-Perot changing linearly with phase of silicon, so it is more suitable for our design purpose in the desired range of measurements than the other one.
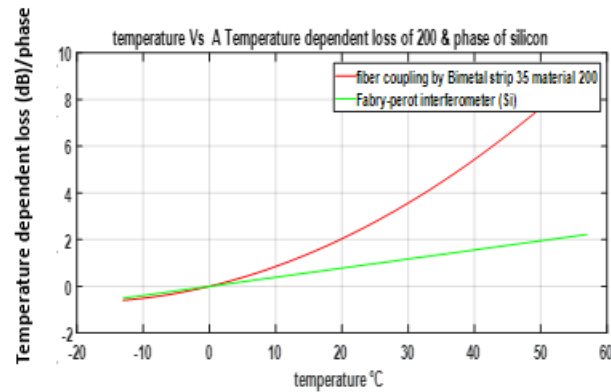

Figure 15: Comparison between two devices.

5   Conclusions

Two different types of fiber optic temperature sensors have been designed and studied. The two sensors were specially designed to be able to measure the temperature range (-13 ℃ to 57.8 ℃) that is well suited for Libyan environment. These types of fiber optics sensor are usually used in high power generators rooms, where the explosion risk factor is very high with the using of regular electric sensors. The first device is based on the Fabry-Perot interferometer with the material of silicon. The optimum designed length obtained is 20.7μm for the operating wavelength of 1550nm. The second device designed is based on fiber coupling actuated by a bimetal strip. The designed length, delta deflection and thickness for the strip were found to be 5.6μm, 35μm and 1.3μm respectively.

From the simulation results, it is clear that the Fabry-Perot temperature sensor of silicon material changes linearly with phase while the sensor based fiber coupling by bimetal strip is not changing linearly with power loss, which would give less measuring accuracy and it is also more difficult to calibrate, however, it is more cheaper than Fabry-Perot sensor.

References

[1]   G. Beheim, "Fiber-Optic Thermometer Using Semiconductor-Etalon Sensor," Electron. Lett. 22, 238-239 (1985).

[2]   Fabry-Pérot Interferometer. Available online:
       http://en.wikipedia.org/wiki/Fabry%E2%80%93P%C3%A9rot_interferometer,22/8/2017.

[3]   K. Kyuma, S. Tai, T. Sawada and M. Nunoshita, "Fiber-Optic Instrument for Temperature Measurement," IEEE J. Quantum Electron. QE-18, 676 (1982).

[4]   Kim, S.H.; Lee, J.J., Lee, D.C., Kwon, I.B. A study on the development of transmission-type extrinsic Fabry-Perot interferometric optical fiber sensor. J. Lightw. Techol. 1999, 17, 1869-1874.

[5]   L. Schultheis, H. Amstutz, and M. Kaufmann, "Fiber-Optic Temperature Sensing With Ultrathin Silicon Etalons," Opt. Lett. 13, 782 (1988).

[6]   Fu, H.Y.; Tam, H.Y.; Shao, L.Y.; Dong, X.; Wai, P.K.A.; Lu, C.; Khijwania, S.K. Pressure sensor realized with polarization-maintaining photonic crystal fiber-based Sagnac interferometer. Appl. Opt. 2008, 47, 2835-2839.

[7]   Glenn Beheim, Fiber-Optic Temperature Sensor Using a Thin-film Fabry-PerotInterferometer , Ph.D. thesis, Case Western Reserve University, Cleveland, Ohio, May 1996.

[8]   Johan Jason,"Theory and Applications of Coupling Based Intensity Modulated Fibre-Optic Sensors", Mid Sweden University,2008.